PAPER

Fe$_3$O$_4$/PANI/CuI as a sustainable heterogeneous nanocatalyst for A^3 coupling†

Nisha,[a] Sahil Kohli,[bg] Snigdha Singh,[a] Neera Sharma*[c] and Ramesh Chandra [ID] *[adef]

The prepared copper iodide nanoparticles were impregnated on the support of ferrite nanoparticles functionalized with polyaniline, resulting in a magnetically recoverable heterogeneous nanocomposite. The activity of the prepared nanocomposite was investigated in the synthesis of propargylamine derivatives *via* A^3 coupling under mild conditions. Techniques such as FESEM, EDAX, XRD, XPS, TEM, BET and FTIR were used to characterize the effective and unique heterogeneous Fe$_3$O$_4$/PANI/CuI nanocomposite developed in this work. This method used in the current study has several advantages, including a short reaction time, neat conditions, good product yield, ideal green matrices values, reusability for up to seven cycles, and magnetic retrievability.

Introduction

Magnetic nanoparticles (MNPs) are of great importance due to their various applications in catalysis, magnetic resonance imaging (MRI), magnetic fluids, and biotechnology.[1] MNPs can serve as magnetically recoverable catalysts for a variety of catalytic reactions because of their insoluble and paramagnetic character, which allows for easy separation from the reaction medium. Moreover, magnetic separation has evolved into one of the most significant and well-known catalytic methods in organic chemistry without the need for filtering, centrifugation, or other laborious workup procedures, simply by using an external magnet.[2] However, bare MNPs have some limitations such as the tendency to easily agglomerate, colloidal instability, and dissolution in acids.[3] The colloidal instability of MNPs leads to their agglomeration due to magnetic dipole–dipole interaction.[4,5] This issue can be resolved by surface functionalization of MNPs using protective shells or coatings such as silica, carbon, or organic polymers.[3] Furthermore, these coatings allow the covalent attachment of organic compounds on distinct nanoparticles, facilitating applications such as drug carriers, heterogeneous catalysis, and absorption media.[3] The magnetic nature of nanoparticles permits facile recovery of nanocatalysts from reaction mixtures through magnets.[5]

One of the polymeric shells synthesized *via* oxidative polymerization is polyaniline (PANI).[6] The choice of polyaniline is because of its various properties such as facileness of synthesis, conductivity as a polymer, low cost, and a porous structure that can enhance the catalytic activity of nanoparticles. The Fe$_3$O$_4$/PANI hybrid shell can be considered a multifunctional support for metal nanocatalysts with significant catalytic performance.[7]

The benefits of a metal nanoparticle supported on nano-size heterogeneous material include good selectivity, minimal accumulation of metal nanoparticles, high dispersion in a liquid medium, and excellent reusability.[8] Copper-based nanoparticles not only enhance the physicochemical characteristics of the nanoparticles but also reinforce the interface between the metal and the support.[9] Cu-based nanocatalysts have abundant applications in nanotechnology due to their special properties and features such as catalysing organic transformations, electrocatalysis, and photocatalysis.[10] Supported copper nanoparticles, such as CuO/NiO,[9] CuO/Al$_2$O$_3$,[11] ZnO/CuI/PPy,[12] and Cu–MgO,[13] have been used in many organic transformations. Copper-based nanocatalysts are found to be useful in various reactions including C–H activation of alkynes, oxygen arylation reaction, Suzuki reaction, Click reaction, Knoevenagel condensation-Michael addition cyclization reaction, Heck reaction and producing copper-acetylated species *in situ* to afford propargylamines.[14]

Propargylamines are crucial building blocks for organic synthesis because they can be utilized as synthetic precursors for synthesizing various medicinally essential compounds.[8] Propargylamines are formed *via* a three-component reaction known as A^3 coupling, which comprises a terminal alkyne, an aldehyde, and an amine.[15] Moreover, a variety of

[a]Drug Discovery & Development Laboratory, Department of Chemistry, University of Delhi, Delhi-110007, India. E-mail: acbrdu@hotmail.com

[b]Department of Chemistry, School of Basic Sciences, Galgotias University, Greater Noida-203201, Uttar Pradesh, India

[c]Department of Chemistry, Hindu College, University of Delhi, Delhi-110019, India

[d]Dr. B. R. Ambedkar Centre for Biomedical Research (ACBR), University of Delhi, Delhi-110007, India

[e]Institute of Nanomedical Science (INMS), University of Delhi, Delhi-110007, India

[f]Maharaja Surajmal Brij University, Bharatpur-321201, Rajasthan, India

[g]Manav Rachna International Institute of Research & Studies, Faridabad, Haryana-121004, India

† Electronic supplementary information (ESI) available. See DOI: https://doi.org/10.1039/d4na00448e
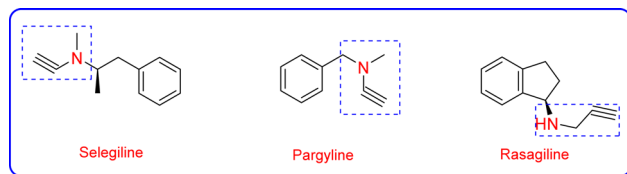
Fig. 1 Examples of approved drugs containing propargylamine skeletons.

propargylamines have been used to cure neuropsychiatric conditions like anxiety, Parkinson's disease, and depression.[16] Various approved drugs, such as pargyline, selegiline, and rasagiline (Fig. 1), have a propargylamine scaffold.[8,17] Late transition metals such as Au, Cu, and Ag are used to catalyse A^3 reactions *via* one-pot synthesis.[18]

Over the past two decades, a catalytic variation of A^3 coupling has attracted chemists' attention[15] A^3 coupling catalysed by various nanocatalysts such as Fe_3O_4@*R. tinctorum*/Ag,[19] Cu/C,[16] Fe_3O_4@SiO_2@DNHCS-Tr@CuI,[20] Au nanoparticles,[21] Fe_3O_4–MoO_3 (ref. 22) and CuO/GNS[23] have been reported. However, these methods involve use of harmful reagents, prolonged reaction time, use of additives and costly reagents. Hence, there is a need for a sustainable heterogeneous nanocatalyst for the facile synthesis of propargylamines *via* A^3 coupling.

In the current work, we successfully develop a novel heterogeneous nanocatalyst, Fe_3O_4/PANI/CuI, for the synthesis of propargylamines *via* A^3 coupling using pyrrolidine, phenylacetylene, and different benzaldehydes under neat conditions at 80 °C in a N_2 atmosphere. The reaction was completed in 10 min with a high yield of the desired product. The fabricated nanocatalyst was easily recoverable and reusable with high catalytic efficiency for the synthesis of propargylamines.

Results and discussion

Synthesis and characterisation

Synthesis of Fe_3O_4 nanoparticles. Fe_3O_4 nanoparticles were synthesised using the co-precipitation approach. To a 250 mL round bottom flask containing 100 mL of water, 4.2 g of $FeSO_4 \cdot 7H_2O$ and 6.1 g of $FeCl_3 \cdot 6H_2O$ were added. The mixture

was stirred at 80 °C for 1 h. Then, 10 mL of ammonia solution (25%) was added dropwise into the reaction mixture with continuous stirring. Then, the reaction was continuously stirred for another 1.5 h at the same temperature. The Fe_3O_4 nanoparticles were collected using a magnet and washed with water many times and then with ethanol. Finally, the synthesised nanoparticles were dried in an oven at 50 °C.[5]

Synthesis of Fe_3O_4/PANI nanoparticles. The obtained Fe_3O_4 nanoparticles were dispersed in 10 mL of deionized water. Subsequently, 0.3 mL of HCL (0.1 M) and 0.2 mL of aniline were added to this solution. Then, the solution was stirred for 1 h at room temperature. Then, the aqueous solution of ammonium persulfate (5 mL) was poured dropwise to the above reaction under ultrasonic irradiation. The stirring was then continued for 3 h in an ice bath. Then, nanoparticles were collected with a magnet and then washed many times with water and three times with ethanol, and further dried in an oven at 50 °C.

Synthesis of Fe_3O_4/PANI/CuI nanoparticles. The prepared Fe_3O_4/PANI nanoparticles were dispersed in water *via* stirring for 10 min. Then, copper iodide nanoparticles were added to this solution and it was stirred overnight at room temperature.
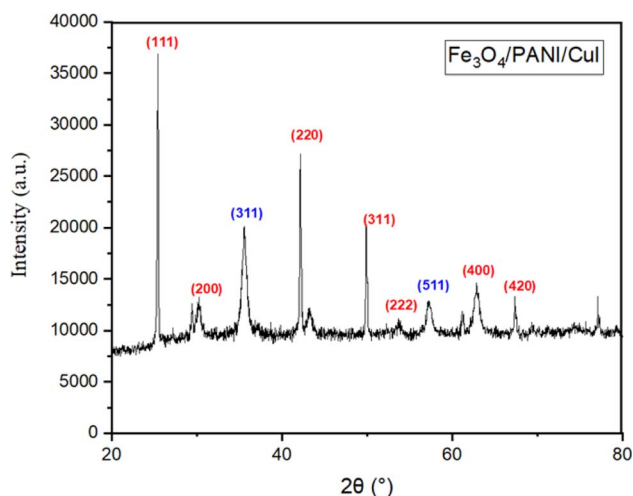

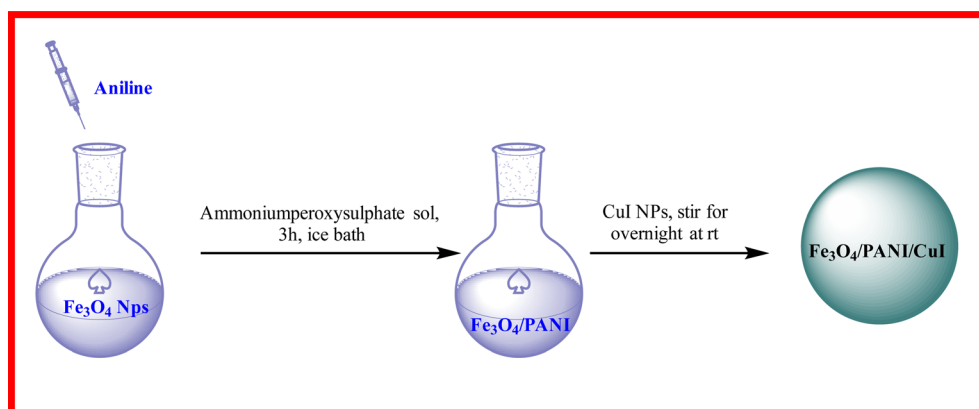Fig. 3 XRD pattern of Fe_3O_4/PANI/CuI nanocatalyst.

Fig. 2 Schematic diagram for the synthesis of nanocomposite.

Then, nanoparticles were washed with water and ethanol and dried in an oven overnight at 50 °C (Fig. 2).

Characterisation of developed Fe_3O_4/PANI/CuI nanocatalyst. X-ray diffraction analysis of the Fe_3O_4/PANI/CuI nanocomposite is shown in Fig. 3. The diffraction angles (2θ) at 35.46° and 57.06° correspond to the crystal planes (311) and (511), respectively, of the Fe_3O_4 nanoparticles.[24,25] The peaks at $2\theta =$ 25.42°, 30.06°, 42.2°, 49.86°, 57.14°, 61.22°, and 67.3° correspond to the crystal planes (200), (311), (111), (420), (222), (220), and (420), respectively, of the cubic phase of CuI.[26]

The field-emission scanning electron microscopy (FESEM) technique reveals the spherical morphology of the nanocomposite (Fig. 4). The transmission electron microscopy (TEM) analysis of the Fe_3O_4/PANI/CuI nanocomposite indicates that CuI is well embedded over the core–shell structure of Fe_3O_4 nanoparticles and the average size of nanoparticles is 42.6 nm, as shown in Fig. 5.

The energy-dispersive X-ray analysis of the Fe_3O_4/PANI/CuI nanocatalyst revealed the presence of iron (42.74 wt%), nitrogen (1.47 wt%), copper (11.7 wt%), oxygen (15.29 wt%), iodine (19.9 wt%), and carbon (8.9 wt%), as can be seen in Fig. 6.

Fig. 7 illustrates the X-ray photoelectron spectra (XPS) of the Fe_3O_4/PANI/CuI nanocomposite. The spectra revealed the presence of Cu $2p_{1/2}$ and Cu $2p_{3/2}$ with binding energies at 952.88 and 932.44 eV, respectively, and the presence of I $3d_{3/2}$ and $3d_{5/2}$ with binding energies at 631 and 619.23 eV, respectively. The values for copper and iodine resemble the reported binding energy values of CuI, which confirm the +1 oxidation state of copper in the nanocomposite.[27] The peak at 284.78 eV corresponds to the binding energy value of C 1s. The values of binding energies at 724.53 and 710.63 eV resemble the reported values of Fe $2p_{3/2}$ and Fe $2p_{1/2}$, respectively, while the peak at 530.17 eV corresponds to O 1s, confirming the presence of Fe_3O_4 in the nanocomposite. The broadness of the iron peaks indicates the presence of both oxidation states (Fe^{2+} and Fe^{3+}) in Fe_3O_4.[28]

Fig. 8 shows the FTIR spectrum of Fe_3O_4/PANI/CuI; it depicts a peak at 3311 cm^{-1}, which is attributed to the presence of the surface OH group in the nanocomposite.[29] The peaks at 1598 and 1494 cm^{-1} are attributed to the C=C stretching vibrations of a quinoid and benzenoid ring, respectively.[30] A peak that appeared at 1374 cm^{-1} is similarly typical of polyaniline and is considered to be a consequence of C–N stretching vibrations
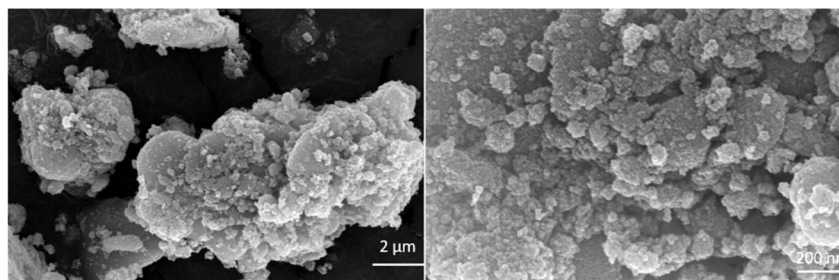

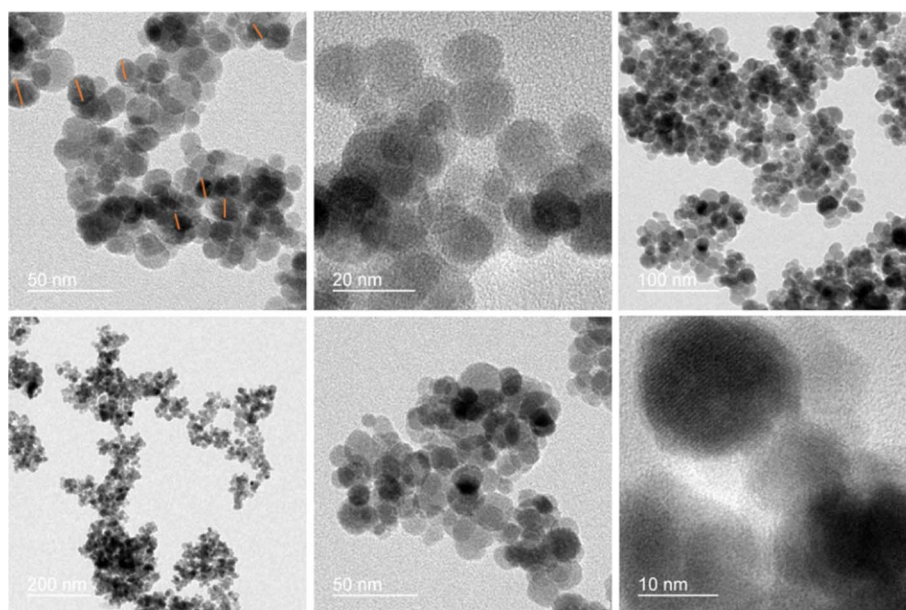Fig. 4 FESEM analysis of Fe_3O_4/PANI/CuI nanocatalyst.
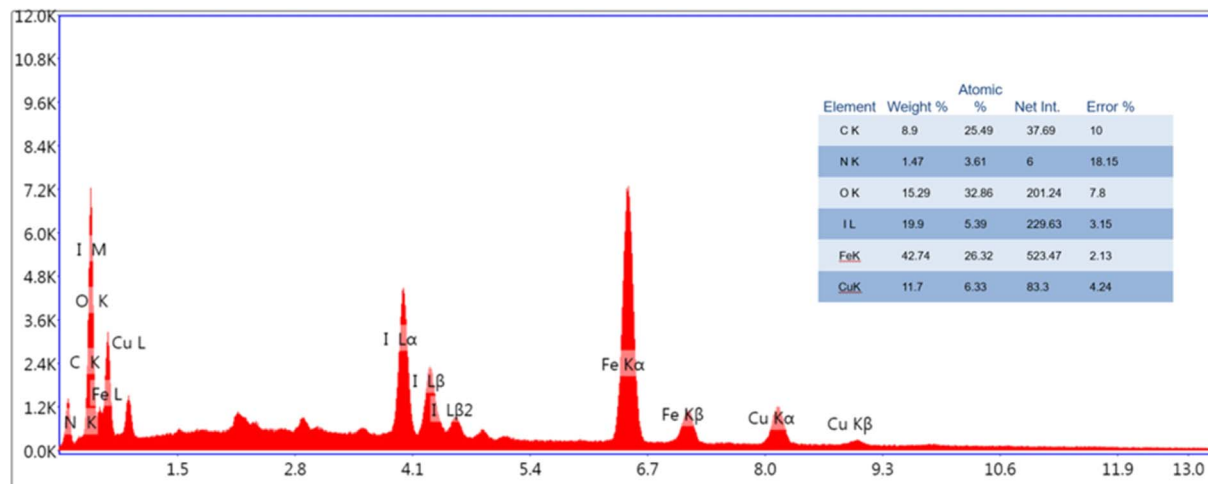

Fig. 5 TEM analysis of Fe_3O_4/PANI/CuI nanocatalyst.

Fig. 6 EDAX analysis of Fe$_3$O$_4$/PANI/CuI nanocatalyst.
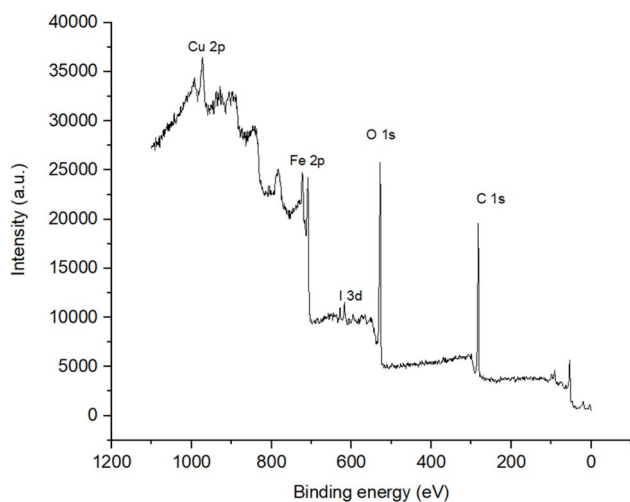
Fig. 7 XPS of Fe$_3$O$_4$/PANI/CuI nanocatalyst.

Fig. 8 FTIR of Fe$_3$O$_4$/PANI/CuI nanocatalyst.

near a quinonoid ring.[31] The peak at 1161 cm^{-1} is due to the C–N stretching vibration.[30] The peak at 553 cm^{-1} is the characteristic peak of ferrite nanoparticles.[30]

N$_2$-Adsorption desorption isotherm was collected using the Brunauer–Emmett–Teller (BET) technique, which is portrayed as a H3 hysteresis loop of isotherm and shows a surface area of 38.471 m^2 g^{-1}, pore radius of 2.16 nm, and pore volume of 0.076 cm^3 g^{-1} (Fig. 9).

Fe$_3$O$_4$/PANI/CuI as heterogeneous nanocatalysts for the synthesis of propargylamine derivatives

We synthesized propargylamine derivatives using Fe$_3$O$_4$/PANI/CuI to investigate its catalytic properties in organic transformations (Scheme 1). For optimization, a model reaction was performed involving phenylacetylene (**1**), pyrrolidine (**2**), and 4-methyl benzaldehyde (**3**) using the nanocatalyst in various solvents or under neat conditions at 80 °C in a nitrogen atmosphere for the preparation of the desired product **4b**, as shown
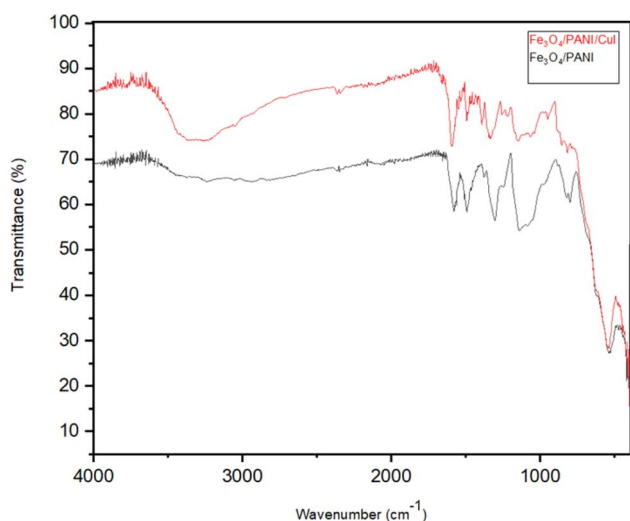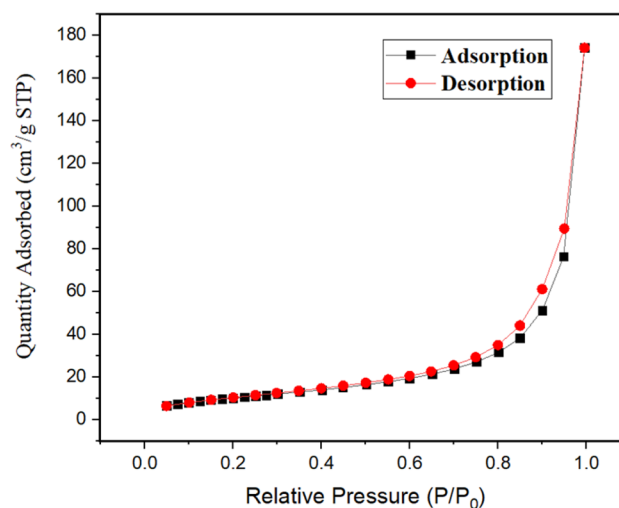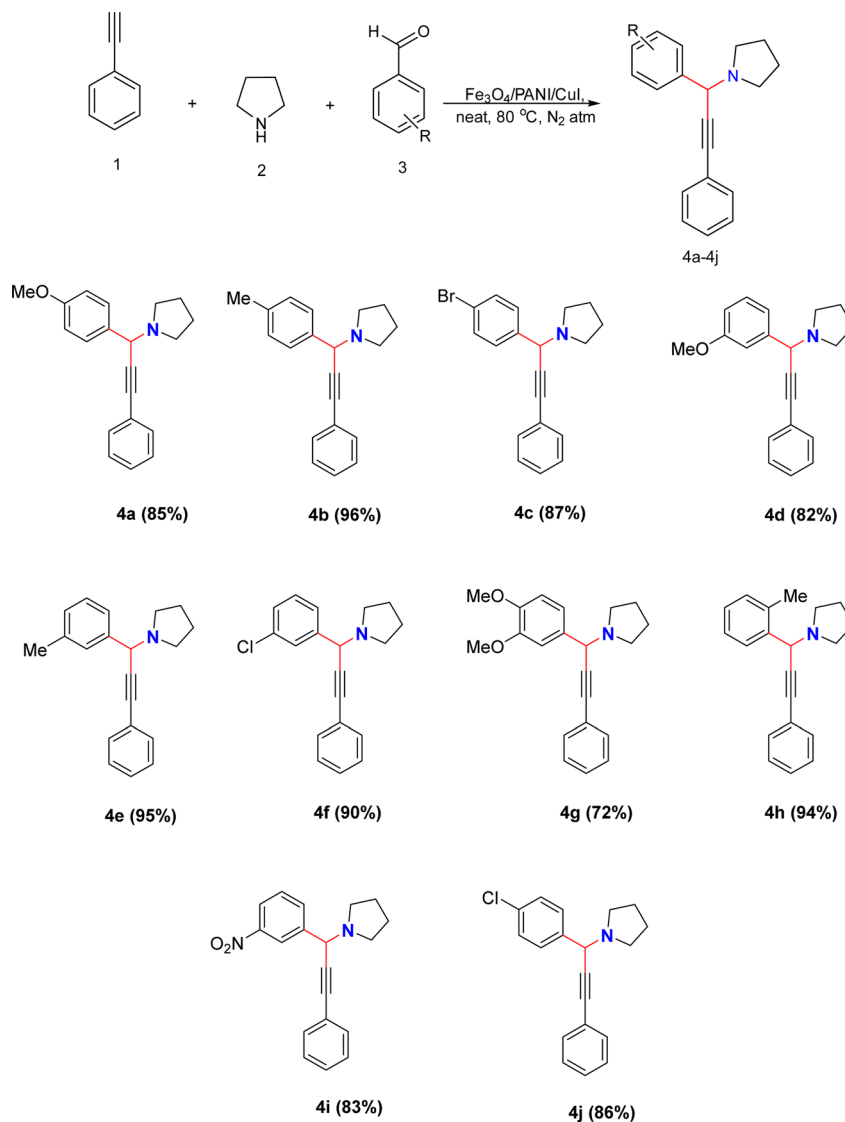

**Fig. 9** N$_2$ adsorption–desorption isotherm of nanocatalyst.

Scheme 1 Fe_3O_4/PANI/CuI catalysed synthesis of propargyl derivatives *via* A^3 coupling. Reaction conditions: nanocatalyst (10 mg), phenylacetylene (1 mmol), pyrrolidine (1 mmol), aromatic aldehyde (1 mmol), neat, 80 °C, N_2 atm, 10 min.

in Table 1. We examined how different catalyst loading amounts, solvent concentrations, and temperatures affected the reaction kinetics, as presented in Table 1. Initially, the model reaction was performed in toluene (Table 1, entry 1), resulting in a 47% yield of the product. Subsequently, the reaction was carried out in polar aprotic solvents such as THF, acetonitrile, DMSO, and DMF. The desired product did not form in both acetonitrile and THF (Table 1, entries 2 and 3). However, the product was obtained with a 40% yield in DMF (Table 1, entry 4). The reaction was then monitored in environmentally friendly solvents such as ethanol, water, and ethylene glycol (EG), yielding no product in water (Table 1, entry 5), trace amounts of product in ethanol, and 30% product yield in EG (Table 1, entry 7). The product was isolated in good yield in neat conditions (Table 1, entry 8). By altering the catalyst loading, the % yield was found to remain unchanged on lowering or increasing the catalyst amount respectively (Table 1, entries 9 and 10). Further, we studied the influence of temperature on

development of reaction. On raising the temperature, there was no change in product yield (Table 1 entry 11), while on decreasing the temperature, there was a reduction in the product yield (Table 1, entry 12).

Under optimized conditions, we examined the recyclability of the catalyst to produce the product **4b**. Once the reaction was completed, the catalyst was recovered from the reaction using a magnet and then washed many times with water and ethanol before being dried in the oven. The recovered catalyst was then used for seven cycles (Fig. 10). The stability of the recycled catalyst after seven cycles was confirmed by XRD, SEM, FTIR, EDAX and TEM, which confirmed that there was no change in the activity and morphology of the catalyst (ESI Fig. S1–S5†). An ICP study of the filtrate was done after catalyst recovery and showed the leached metal concentrations of copper and iron ion to be 2.08 and 0.12 ppm, respectively, which are lower than the authentic values of the respective ions according to WHO terms.[32]

Table 1 Optimization of nanocatalyst for the synthesis of propargyl derivatives *via* A^3 coupling using phenyl acetylene (**1**), pyrrolidine (**2**), and 4-methylbenzaldehyde (**3**)^a
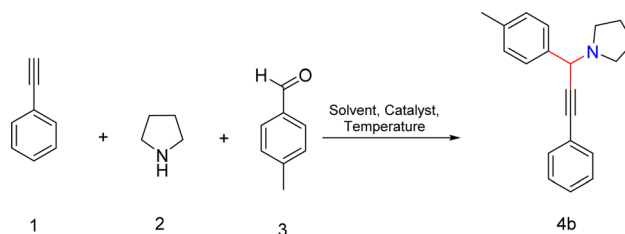
S. no.	Nanocatalyst (mg)	Solvent	Temp. (°C)	Time (min)	Yield (%)
1	Fe$_3$O$_4$/PANI/CuI (10)	Toluene	80	10	47
2	Fe$_3$O$_4$/PANI/CuI (10)	CH$_3$CN	80	10	—
3	Fe$_3$O$_4$/PANI/CuI (10)	THF	80	10	—
4	Fe$_3$O$_4$/PANI/CuI (10)	DMF	80	10	40
5	Fe$_3$O$_4$/PANI/CuI (10)	Water	80	10	—
6	Fe$_3$O$_4$/PANI/CuI (10)	Ethanol	80	10	Trace
7	Fe$_3$O$_4$/PANI/CuI (10)	EG	80	10	30
8	**Fe$_3$O$_4$/PANI/CuI (10)**	**Neat**	**80**	**10**	**96**
9	Fe$_3$O$_4$/PANI/CuI (5)	Neat	80	10	53
10	Fe$_3$O$_4$/PANI/CuI (20)	Neat	80	10	96
11	Fe$_3$O$_4$/PANI/CuI (10)	Neat	110	10	96
12	Fe$_3$O$_4$/PANI/CuI (10)	Neat	50	10	22
13	CuI (10)	Neat	80	10	41

^{a} Reaction conditions: catalyst (5–20 mg), **1** (1.0 mmol), **2** (1 mmol), **3** (1 mmol), solvent (2–3 mL), N$_2$ atm, 80 °C, 10 min.
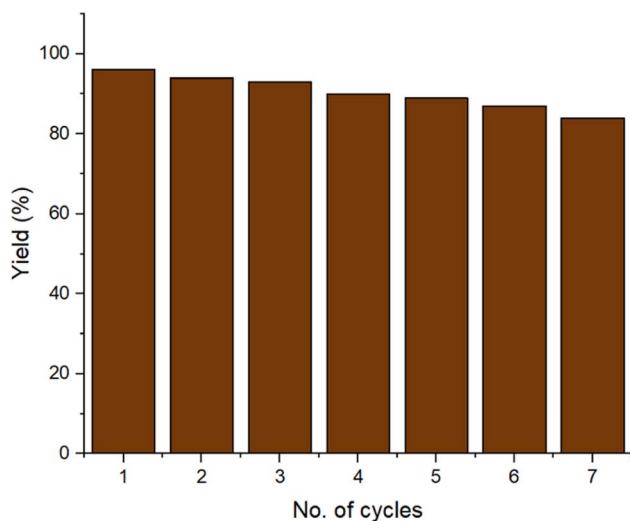
Fig. 10 Catalyst recyclability test.

The existing methodology demonstrates sustainability and eco-friendliness, as evidenced by the green metrics values, as shown in Table 2 (refer to calculations in the ESI†), which closely approach the ideal values.

Table 3 provides a summary of the literature review, listing the previously established methods for producing propargyl derivatives, including the reaction conditions and corresponding yields.

The plausible mechanism for the synthesis of propargylamine *via* A^3 coupling catalysed by the Fe$_3$O$_4$/PANI/CuI nanocomposite is shown in Fig. 11. The copper-based nanocatalyst activates the phenylacetylene ring and proceeds through an attack on the carbon of the iminium ion, which is formed from the aldehyde and amine and results in the formation of the desired product as well as catalyst regeneration.[33,39]

General procedure for the synthesis of propargyl derivatives

In general, a mixture of phenylacetylene (1 mmol), pyrrolidine (1 mmol), aromatic aldehyde (1 mmol), and catalyst (10 mg) was added to a 50 mL round-bottom flask and stirred continuously at 80 °C. TLC was used to monitor the progress of the reaction. After the completion of the reaction, the reaction mixture was cooled and diluted with ethyl acetate, and the catalyst was separated with the aid of a magnet. The crude product was extracted with ethyl acetate and purified by column chromatography using basic alumina as a stationary phase and ethyl

Table 2 Green matrices values

Catalyst	Reaction mass efficiency	E-Factor	Process mass intensity	Carbon efficiency
Fe$_3$O$_4$/PANI/CuI	90%	0.10	1.10	96%

Table 3 Comparative analysis of various catalysts for the synthesis of propargylamine derivatives

S. no.	Nanocatalyst	Reaction conditions	Time	% Yield	Ref.
1	Fe_3O_4@SiO_2–Se-T/CuI	Neat, 80 °C	2 h	95	33
2	ZSM-5/APTMS/(E)-4-((pyridine-2-ylimino)methyl)benzaldehyde/Cu-NPs	K_2CO_3, H_2O, 60 °C	2 h	94	34
3	UIO-66-NH_2G1@PdNPs	Toluene, N_2 gas, 110 °C	3 h	93	35
4	[Fe_3O_4@bisimidazolium-Pd]$^{2Cl^-}$	PEG-400, 100 °C	2 h	98	36
5	Fe_3O_4@starch-Acr@Cu(II)	H_2O, reflux	35 min	99	37
6	g-C_3N_4-TCT-2AEDSEA-Ag-Cu-Ni	Toluene, 80 °C	8 h	91	38
7	Fe_3O_4@SiO_2-di-(pyridin-2-yl)amine-Cu	H_2O, reflux	2 h	99	39
8	Co^{2+}-Cu@SA(0)-600	Toluene, 110 °C	1 h	89	40
9	MMT-K10/Fe_3O_4/CuO	Toluene, 80 °C	8 h	91	41
10	o-Cu_2O-PVP	Neat, 100 °C	5 min	80	42
11	**Fe_3O_4/PANI/CuI**	**Neat, 80 °C**	**10 min**	**96**	**Our work**
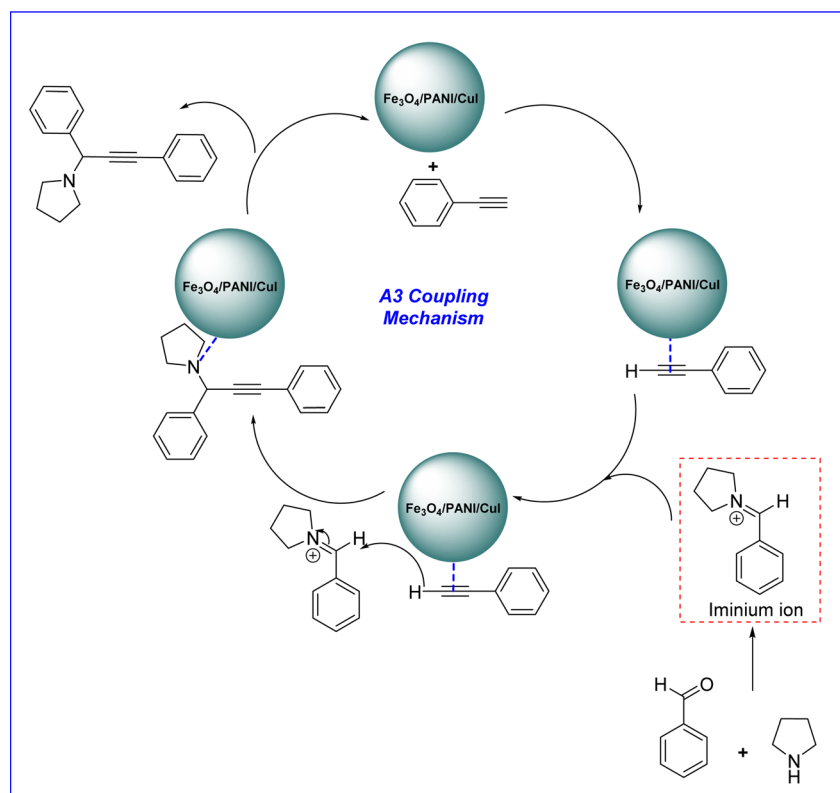
Fig. 11 Mechanism for Fe_3O_4/PANI/CuI catalysed synthesis of propargylamine derivative via A^3 coupling.

acetate : hexane as an eluent. The obtained pure product was confirmed by ^1H and ^{13}C NMR spectroscopy.

Conclusion

In summary, we have developed a sustainable heterogeneous copper-based magnetic nanocatalyst for the one-pot synthesis of propargylamine derivatives under solvent-free conditions with a short reaction time. The designed nanocatalyst is easily magnetically recoverable and can be recycled for up to seven runs without any drastic reduction in product yield. This protocol provides a shorter reaction time to obtain products with high yield and good catalytic activity under mild reaction conditions as compared to previously reported methods.

Data availability

The data that support the findings of this study are available from the corresponding author following reasonable request.

Conflicts of interest

The authors declare no conflicts of interest.

Acknowledgements

References

1 A. H. Lu, E. E. Salabas and F. Schuth, Magnetic nanoparticles: synthesis, protection, functionalization, and application, *Angew. Chem., Int. Ed.*, 2007, **46**(8), 1222–1244.

2 M. Abedi, M. Hosseini, A. Arabmarkadeh and M. Kazemi, Magnetic nanocatalysts in A3-coupling reactions, *Synth. Commun.*, 2021, **51**(6), 835–855.

3 T. E. Saraswati, A. Ogino and M. Nagatsu, Plasma-activated immobilization of biomolecules onto graphite-encapsulated magnetic nanoparticles, *Carbon*, 2012, **50**(3), 1253–1261.

4 S. P. Yeap, J. Lim, B. S. Ooi and A. L. Ahmad, Agglomeration, colloidal stability, and magnetic separation of magnetic nanoparticles: collective influences on environmental engineering applications, *J. Nanopart. Res.*, 2007, **19**(11), 1–15.

5 (a) R. A. Bohara, N. D. Thorat and S. H. Pawar, Role of functionalization: strategies to explore potential nano-bio applications of magnetic nanoparticles, *RSC Adv.*, 2016, **6**(50), 43989–44012; (b) S. Singh, T. Goel, A. Singh, H. Chugh, N. Chakraborty, I. Roy, M. Tiwari and R. Chandra, Synthesis and characterization of Fe₃O₄@SiO₂@PDA@Ag core–shell nanoparticles and biological application on human lung cancer cell line and antibacterial strains, *Artif. Cells, Nanomed., Biotechnol.*, 2024, **52**(1), 46–58; (c) M. Kazemi and M. Mohammadi, Magnetically recoverable catalysts: catalysis in synthesis of polyhydroquinolines, *Appl. Organomet. Chem.*, 2020, **34**(3), e5400.

6 (a) J. P. L. Morais, D. V. Bernardino, B. d. S. Batista, W. O. Pereira, F. M. B. Amaral, M. C. M. P. Branca and F. P. Gasparin, Conductive polymer blend based on polyaniline and galactomannan: optical and electrical properties, *Synth. Met.*, 2023, **295**, 117346; (b) S. Kohli, G. Rathee, S. Hooda and R. Chandra, Al₂O₃/CuI/PANI nanocomposite catalyzed green synthesis of biologically active 2-substituted benzimidazole derivatives, *Dalton Trans.*, 2021, **50**(22), 7750–7758.

7 (a) J. Chenjing, H. Jie, C. Fangyuan, W. Xiaoxia and G. Rong, Fe₃O₄@PANI hybrid shell as a multifunctional support for Au nanocatalysts with a remarkably improved catalytic performance, *Langmuir*, 2017, **33**, 4520–4527; (b) Nisha, S. Kohli, N. Sharma and R. Chandra, Development of ZnO/PANI/Ag nanocomposite for synthesis of bioactive xanthene-1, 8 (2H)-dione derivatives, *Appl. Organomet. Chem.*, 2023, **37**, e7049.

8 (a) E. Zarenezhad, R. Taghavi, P. Kamrani, M. Farjam and S. Rostamnia, Gold nanoparticle decorated dithiocarbamate modified natural boehmite as a catalyst for the synthesis of biologically essential propargylamines, *RSC Adv.*, 2022, **12**(49), 31680–31687; (b) P. Munnik, P. E. De Jongh and K. P. De Jong, Recent developments in the synthesis of supported catalysts, *Chem. Rev.*, 2015, **115**(14), 6687–6718; (c) M. Mohammadi, M. Khodamorady, B. Tahmasbi, K. Bahrami and A. Ghorbani-Choghamarani, Boehmite nanoparticles as versatile support for organic–inorganic hybrid materials: synthesis, functionalization, and applications in eco-friendly catalysis, *J. Ind. Eng. Chem.*, 2021, **97**, 1–78; (d) X. Zheng, P. Li, S. Dou, W. Sun, H. Pan, D. Wang and Y. Li, Non-carbon-supported single-atom site catalysts for electrocatalysis, *Energy Environ. Sci.*, 2021, **14**(5), 2809–2858.

9 M. Rawat and D. S. Rawat, CuO@NiO nanocomposite catalyzed synthesis of biologically active indenoisoquinoline derivatives, *ACS Sustain. Chem. Eng.*, 2020, **36**, 13701–13712.

10 N. K. Ojha, G. V. Zyryanov, A. Majee, V. N. Charushin, O. N. Chupakhin and S. Santra, Copper nanoparticles as inexpensive and efficient catalyst: A valuable contribution in organic synthesis, *Coord. Chem. Rev.*, 2017, **353**, 1–57.

11 S. Khan, S. S. Shah, N. K. Janjua, A. B. Yurtcan, M. T. Nazir, K. M. Katubi and N. S. Alsaiari, Alumina supported copper oxide nanoparticles (CuO/Al₂O₃) as high-performance electrocatalysts for hydrazine oxidation reaction, *Chemosphere*, 2023, 137659.

12 S. Kohli, Nisha, G. Rathee, S. Hooda and R. Chandra, Exploring the untapped catalytic application of a ZnO/CuI/PPy nanocomposite for the green synthesis of biologically active 2,4,5-trisubstituted imidazole scaffolds, *Nanoscale Adv.*, 2023, **5**(8), 2352–2360.

13 K. N. Patil, P. Manikanta, R. R. Nikam, P. M. Srinivasappa, A. H. Jadhav, H. P. Aytam, K. S. R. Rao and B. M. Nagaraja, Effect of precipitating agents on activity of co-precipitated Cu–MgO catalysts towards selective furfural hydrogenation and cyclohexanol dehydrogenation reactions, *Results Eng.*, 2023, **17**, 100851.

14 (a) S. Cao, B. Zou, J. Yang, J. Wang and H. Feng, Hollow CuO–CeO₂ Nanospheres for an effectively catalytic annulation/A³-coupling reaction sequence, *ACS Appl. Nano Mater.*, 2022, **5**(8), 11689–11698; (b) M. J. Ndolomingo, N. Bingwa and R. Meijboom, Review of supported metal nanoparticles: synthesis methodologies, advantages and application as catalysts, *J. Mater. Sci.*, 2020, **55**(15), 6195–6241; (c) F. Ghobakhloo, D. Azarifar, M. Mohammadi, H. Keypour and H. Zeynali, Copper (II) Schiff-base complex modified UiO-66-NH₂ (Zr) metal–organic framework catalysts for Knoevenagel condensation–Michael addition–cyclization reactions, *Inorg. Chem.*, 2022, **61**(12), 4825–4841.

15 B. V. Rokade, J. Barker and P. J. Guiry, Development of and recent advances in asymmetric A3 coupling, *Chem. Soc. Rev.*, 2019, **48**(18), 4766–4790.

16 P. V. Rathod, J. M. C. Puguan and H. Kim, Solvent-free synthesis of propargyl amines via A³ coupling reaction and organic pollutant degradation in aqueous condition using Cu/C catalyst, *Appl. Organomet. Chem.*, 2020, **34**(12), e5986.

17 O. Weinreb, T. Amit, O. Bar-Am and M. B. Youdim, Rasagiline: a novel anti-Parkinsonian monoamine oxidase-

B inhibitor with neuroprotective activity, *Prog. Neurobiol.*, 2010, **92**(3), 330–344.

18 J. Farhi, I. N. Lykakis and G. E. Kostakis, Metal catalysed A^3 coupling methodologies: classification and visualization, *Catalysts*, 2022, **12**, 660.

19 H. Veisi, L. Mohammadi, S. Hemmati, T. Tamoradi and P. Mohammadi, *In situ* immobilized silver nanoparticles on *Rubia tinctorum* extract-coated ultrasmall iron oxide nanoparticles: an efficient nanocatalyst with magnetic recyclability for synthesis of propargylamines by A^3 coupling reaction, *ACS Omega*, 2019, **4**(9), 13991–14003.

20 S. Peiman, R. Baharfar and R. Hosseinzadeh, CuI NPs immobilized on a ternary hybrid system of magnetic nanosilica, PAMAM dendrimer and trypsin, as an efficient catalyst for A^3-coupling reaction, *Res. Chem. Intermed.*, 2022, **48**(4), 1365–1382.

21 M. Kidwai, V. Bansal, A. Kumar and S. Mozumdar, The first Au-nanoparticles catalyzed green synthesis of propargylamines *via* a three-component coupling reaction of aldehyde, alkyne and amine, *Green Chem.*, 2007, **9**(7), 742–745.

22 M. B. Gawande, P. S. Branco, I. D. Nogueira, C. A. A. Ghumman, N. Bundaleski, A. Santos, O. M. Teodoro and R. Luque, Catalytic applications of a versatile magnetically separable Fe–Mo (nanocat-Fe–Mo) nanocatalyst, *Green Chem.*, 2013, **15**(3), 682–689.

23 M. Gopiraman, D. Deng, S. Ganesh Babu, T. Hayashi, R. Karvembu and I. S. Kim, Sustainable and versatile CuO/GNS nanocatalyst for highly efficient base free coupling reactions, *ACS Sustain. Chem. Eng.*, 2015, **3**(10), 2478–2488.

24 A. G. Karunanayake, C. M. Navarathna, S. R. Gunatilake, M. Crowley, R. Anderson, D. Mohan and T. Mlsna, Fe_3O_4 nanoparticles dispersed on Douglas fir biochar for phosphate sorption, *ACS Appl. Nano Mater.*, 2019, **2**(6), 3467–3479.

25 V. A. J. Silva, P. L. Andrade, M. P. C. Silva, L. D. L. S. Valladares and J. A. Aguiar, Synthesis and characterization of Fe_3O_4 nanoparticles coated with fucan polysaccharides, *J. Magn. Magn. Mater.*, 2013, **343**, 138–143.

26 M. Rawat and D. S. Rawat, $CuI@Al_2O_3$ catalyzed synthesis of 2-aminonicotinonitrile derivatives under solvent free condition, *Tetrahedron Lett.*, 2019, **60**(16), 1153–1157.

27 X. Wang, Y. Shen, A. Xie, L. Qiu, S. Li and Y. Wang, Novel structure CuI/PANI nanocomposites with bifunctions: superhydrophobicity and photocatalytic activity, *J. Mater. Chem.*, 2011, **21**(26), 9641–9646.

28 S. Kohli, G. Rathee, S. Hooda and R. Chandra, An efficient approach for the green synthesis of biologically active 2,3-dihydroquinazolin-4 (1*H*)-ones using a magnetic EDTA coated copper based nanocomposite, *RSC Adv.*, 2023, **13**(3), 1923–1932.

29 S. Rajendran, R. Pachaiappan, T. K. Hoang, S. Karthikeyan, L. Gnanasekaran, S. Vadivel, M. Soto-Moscoso and M. A. Gracia-Pinilla, CuO-ZnO-PANI a lethal pnp combination in degradation of 4-chlorophenol under visible light, *J. Hazard. Mater.*, 2021, **416**, 125989.

30 J. Alam, U. Riaz and S. Ahmad, Effect of ferrofluid concentration on electrical and magnetic properties of the Fe_3O_4/PANI nanocomposites, *J. Magn. Magn. Mater.*, 2007, **314**, 93–99.

31 J. Marek, J. Vilcakova, N. E. Kazantseva, J. Prokes, M. Trchova and J. Stejskal, Conducting and magnetic hybrid polyaniline/nickel composites, *Synth. Met.*, 2022, **291**, 117165.

32 W. Yang, B. Vogler, Y. Lei and T. Wu, Metallic ion leaching from heterogeneous catalysts: an overlooked effect in the study of catalytic ozonation processes, *Environ. Sci.: Water Res. Technol.*, 2017, **3**(6), 1143–1151.

33 Y. Rangraz, F. Nemati and A. Elhampour, Design, synthesis, and characterization of a novel magnetically recoverable copper nanocatalyst containing organoselenium ligand and its application in the A^3 coupling reaction, *Ind. Eng. Chem. Res.*, 2019, **58**(37), 17308–17318.

34 M. Leila, M. Hosseinifard, M. R. Vaezi and S. Rostamnia, Stabilization of copper nanoparticles onto the double Schiff-base-functionalized ZSM-5 for A^3 coupling reaction catalysis aimed under mild conditions, *RSC Adv.*, 2023, **13**, 4843–4858.

35 C. Mansoureh, H. Alinezhad and S. Ghasemi, Post-synthetic modification of UIO-66-NH_2 as a highly efficient and recyclable nanocatalyst in the three-component coupling (A^3) reaction for the synthesis of propargylamine derivatives, *J. Organomet. Chem.*, 2023, **1002**, 122903.

36 H. R. Althomali, M. K. Abbood, F. M. Altalbawy, E. A. M. Saleh, S. S. Abdullaev, A. J. Ibrahim, S. A. Ansari and R. M. R. Parra, A novel nanomagnetic palladium (II) complex of bisimidazolium-based N-heterocyclic carbene an efficient heterogeneous catalyst for A^3 coupling reactions, *J. Mol. Struct.*, 2023, 135911.

37 T. Mahmood, F. Mazhari and M. Mavvaji, Copper (II)-immobilized on starch-coated nanomagnetite as an efficient and magnetically recoverable catalyst for the synthesis of propargyl amines through one-pot A^3 coupling reaction, *Org. Prep. Proced. Int.*, 2023, **55**, 251–264.

38 M. Zarei, I. Mohammadzadeh, K. Saidi and H. Sheibani, Synthesis of Ag–Cu–Ni nanoparticles stabilized on functionalized g–C_3N_4 and investigation of its catalytic activity in the A^3-coupling reaction, *ACS Omega*, 2023, **8**, 18685–18694.

39 S. Ahmad, A. M. Ahmad, O. S. Raed, Z. M. Mustafa, K. W. Ali and A. J. Mohammed, Magnetic nanoparticles modified with di (pyridin-2-yl) amine ligand supported copper complex: a novel and efficient magnetically reusable catalyst for A^3 coupling and CS cross-coupling reactions, *Polycyclic Aromat. Compd.*, 2023, **43**, 4407–4425.

40 M. Kaur, S. Sharma, A. Choudhary and S. Paul, Tuning the catalytic performance of a Cu supported silica modified γ-

Al$_2$O$_3$ nanocatalyst *via* cobalt-doping for A^3-coupling, *React. Chem. Eng.*, 2023, **8**, 2141–2155.

41 H. B. Fatemeh, H. Khabazzadeh, M. Fayazi and M. Rezaeipour, Synthesis of CuO and Cu$_2$O nanoparticles stabilized on the magnetic Fe$_3$O$_4$-Montmorillonite-K10 and

comparison of their catalytic activity in A^3 coupling reaction, *J. Iran. Chem. Soc.*, 2023, **20**, 1439–1456.

42 H. Bao, A. Y. Li, V. Kairouz and A. Moores, Ultra-fast Cu-based A^3-coupling catalysts: faceted Cu$_2$O microcrystals as efficient catalyst-delivery systems in batch and flow conditions, *Can. J. Chem.*, 2022, **100**(3), 217–223.